

Unexpected trend of magnetic order of $3d$ transition-metal monolayers on W(001)

P. Ferriani,^{1,*} S. Heinze,¹ G. Bihlmayer,² and S. Blügel²

¹*Institute of Applied Physics and Microstructure Research Center, University of Hamburg, Jungiusstrasse 11, 20355 Hamburg, Germany*

²*Institut für Festkörperforschung, Forschungszentrum Jülich, 52425 Jülich, Germany*

(Received 3 February 2005; published 25 July 2005)

We report systematic first-principles calculations based on the full-potential linearized augmented plane wave method for $3d$ transition-metal (V, Cr, Mn, Fe, Co, Ni) monolayers on the W(001) surface. We predict that V, Cr, and Mn monolayers exhibit a ferromagnetic ground state, while Fe and Co favor the $c(2 \times 2)$ antiferromagnetic state. This trend is surprising as it is opposite to what was expected from the knowledge of magnetism in ultrathin films and results from strong hybridization at the W interface. In particular, this system is the first case showing antiferromagnetic Co.

DOI: [10.1103/PhysRevB.72.024452](https://doi.org/10.1103/PhysRevB.72.024452)

PACS number(s): 75.70.Ak, 71.15.Mb

Magnetism of ultrathin films has been investigated in great detail within the past 15 years^{1,2} and has led to a thorough understanding of these systems. For magnetic monolayers on (001) oriented nonmagnetic substrates, e.g., Cu, Ag, Au, and Pd, there is the widely accepted consensus on general trends of the transition metals: (i) The magnetic moments of monolayers are considerably enhanced compared to the equivalent bulk systems and (ii) Fe, Co, and Ni are ferromagnets on these substrates while V, Cr, and Mn are $c(2 \times 2)$ antiferromagnets, i.e., a checkerboard arrangement of antiparallel magnetic moments.^{1,3,4} First-principles theory has played a very fruitful role in this field. Capitalizing on the predictive power of this approach trends were outlined and their verification challenged experimentalists. For example, the prediction that V is magnetic on Ag surface was verified by Ortega *et al.*⁵ and the two-dimensional antiferromagnetism of the early transition metals (TM) on various substrates was verified by means of spin-polarized scanning tunneling microscopy.⁶

Recently, experimentalists and theoreticians started to focus on the investigation of $3d$ TM monolayers on W(001). For example, in case of 1 ML Fe on W(001) it was demonstrated univocally that this system exhibits a $c(2 \times 2)$ antiferromagnetic (AFM) order^{7,8} in contradiction to common expectations. For 1 ML Co on W(001) experiments indicate a vanishing net magnetization at temperatures down to 140 K but the reason remains unclear.⁹ The unexpected AFM structure of 1 ML Fe on W(001) and the absence of the magnetization of Co raises the question whether the magnetic order of $3d$ TM monolayers on W(001) behaves differently from our present comprehension. So far no experimental investigations have been carried out for Cr or Mn monolayer on W(001), but the current progress in understanding the growth of $3d$ metals on W(001) lets us expect that these questions will be addressed by a series of experiments in the near future.

In this paper we present systematic first-principles calculations based on density functional theory of $3d$ TM monolayers on W(001). We have found that the early transition metals (V, Cr, and Mn) couple ferromagnetically and the late transition metals (Fe, Co) are $c(2 \times 2)$ antiferromagnets on W(001), while Ni is nonmagnetic. Thus, the trend of mag-

netic order of the (001) oriented monolayers across the transition-metal series is reversed to what was expected from previous investigations on noble-metal and late TM substrates. In particular, this is the first time that Co is predicted to be AFM. Cr on W(001), on the other hand, is ferromagnetic (FM) and thus accessible to spin-polarized photoemission and x-ray magnetic circular dichroism. Our results are even more surprising in view of the fact that 1 ML Fe on W(110) is FM¹⁰ and 1 ML Mn on W(110) is AFM.⁶ Thus, we find that the magnetic structure of the overlayer depends also on the substrate orientation.

We have determined the structural, electronic, and magnetic properties of $3d$ TM monolayers on W(001) by performing first-principles calculations using the full-potential linearized augmented plane wave (FLAPW) method in film geometry, as implemented in the FLEUR code.¹¹ We focus on the magnetic ground-state structure. Since the nearest-neighbor interaction between the $3d$ TM dominates there are only two competing magnetic structures, the $p(1 \times 1)$ FM and the $c(2 \times 2)$ AFM. A pseudomorphic $3d$ TM monolayer on W(001) has been modeled by a symmetric nine layer W slab with the experimental W lattice constant of 5.981 a.u. and an additional $3d$ TM layer on both sides. We have applied the generalized-gradient approximation of Perdew, Burke, and Ernzerhof.¹² The W $5p$ semicore states have been described by local p orbitals added to the LAPW basis set. We have used about 120 basis functions per atom and 36 \mathbf{k}_{\parallel} points in the irreducible wedge of the two-dimensional Brillouin zone.

In order to find the magnetic ground state for each system, we have calculated the total energy as function of the interlayer distance d between the $3d$ TM monolayer and the W surface for the FM and $c(2 \times 2)$ AFM configurations. The obtained equilibrium distances are reported in Table I. The smallest relaxation was found for Mn. This is consistent with the established interpretation that the relaxation is controlled by the d -band filling^{13,14} and it is strong for half-filled bands, while it is small for empty or filled bands. For 1 ML Mn on W(001) in either magnetic configuration, the Mn majority d band is nearly filled and the minority d band is nearly empty, resulting in a large interlayer distance. For the other $3d$ TM monolayers on W(001) the Fermi level is located inside one

TABLE I. Equilibrium distance d between the $3d$ TM monolayers and the W substrate for the $c(2 \times 2)$ AFM and the FM configuration. The corresponding relaxation is given with respect to the substrate bulk interlayer spacing.

		V	Cr	Mn	Fe	Co
AFM	$d(\text{\AA})$	2.66	2.50	2.97	2.58	2.33
AFM	rel.(%)	-11.1	-16.4	-0.8	-13.9	-22.1
FM	$d(\text{\AA})$	2.74	2.56	2.85	2.44	2.23
FM	rel.(%)	-8.3	-14.4	-4.7	-18.5	-25.5

of the spin subbands and strong relaxations occur.

The local magnetic moments of the $3d$ TM monolayers on W(001) are plotted in Fig. 1 for the FM and AFM structures at the relaxed interlayer distances. The overall trend across the $3d$ series follows Hund's first rule. The largest moment is found for Mn and it monotonically decreases towards the beginning and the end of the series. This atomic-like behavior indicates that the magnetism is dominated by the local intra-atomic contribution. A comparison with unsupported monolayers (UML) in the experimental W lattice constant shows that the interaction with the substrate reduces the magnetic moment of the $3d$ TM overlayer. This is due to a significant hybridization of the $3d$ wave functions with the extended $5d$ wave functions of the substrate, a consequence of the increased coordination number of the $3d$ TM atoms. For Ni, the magnetic moment vanishes and the overlayer becomes nonmagnetic.

The magnetism of the overlayer also polarizes the substrate. For the FM configuration, W atoms at the interface are antiferromagnetically coupled to the $3d$ TM monolayer (apart from the case of Co) and carry a moment which is roughly proportional to that of the $3d$ TM. The induced polarization decreases rapidly with distance from the interface into the bulk and is already one order of magnitude lower at the second W layer. The sign of the magnetization oscillates from one W layer to the next, indicating a layered AFM

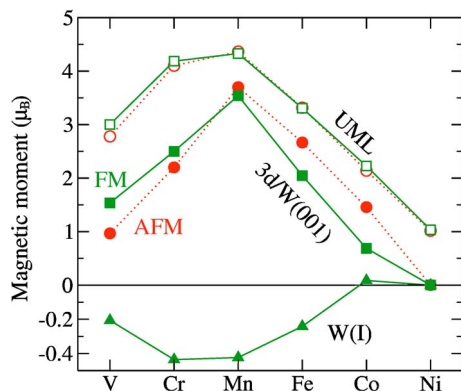


FIG. 1. (Color online) Magnetic moments of the $3d$ TM monolayers on W(001). The $3d$ TM moments are denoted by full green squares (red circles) for the FM (AFM) solution. For the FM case the magnetic moment of interface W atoms is given by triangles. The results for the $3d$ TM UML in the W lattice constant are shown for comparison (open green squares and red circles for the FM and AFM state, respectively).

(LAFM) susceptibility of W(001). The global magnetic structure of the system is therefore a LAFM structure, formed by alternate layers with opposite magnetization direction and layer-dependent size of the moment. For the $c(2 \times 2)$ AFM configuration, on the other hand, due to symmetry reasons the substrate is not magnetized at the interface as well as in every second W layer from the interface.

The key result of this paper is summarized in Fig. 2. The total energy difference $\Delta E = E_{\text{AFM}} - E_{\text{FM}}$ between the $c(2 \times 2)$ AFM and the FM configuration is plotted for $3d$ TM monolayers on various substrates. On W(001), we find that the ground state is FM for V, Cr, and Mn while it is $c(2 \times 2)$ AFM for Fe and Co with large energy differences between the two magnetic solutions. The observed trend across the $3d$ series is rather surprising as it is just the opposite one would have expected from previous studies.^{3,4}

The example of a Pd(001) substrate has been taken from Ref. 3 and included in Fig. 2 for comparison. The trend is indeed inverted with respect to the W(001) substrate with energy differences of similar magnitude. Like the $3d$ TM monolayers on the noble metals, the $3d$ TM monolayers on Pd(001) are examples of two-dimensional magnets. Grown on these substrates, the distances between atoms in the monolayer plane and between the monolayer and the substrate are about the same, but the exchange interaction between the $3d$ - $3d$ atoms in the plane, J_{\parallel} , is much larger than between the atoms in the monolayer and the substrate, J_{\perp} ($J_{\parallel} \gg J_{\perp}$). Thus, there might be two different reasons for the observation of the inverted trend on the bcc W(001) sub-

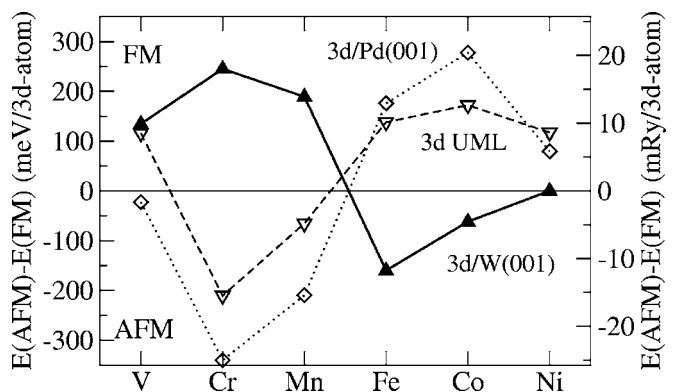


FIG. 2. Total energy difference between $c(2 \times 2)$ AFM and FM configurations for the $3d$ TM monolayers on W(001) (\blacktriangle), on Pd(001) (\diamond), taken from Ref. 3] and without any substrate on the experimental W lattice constant (∇).

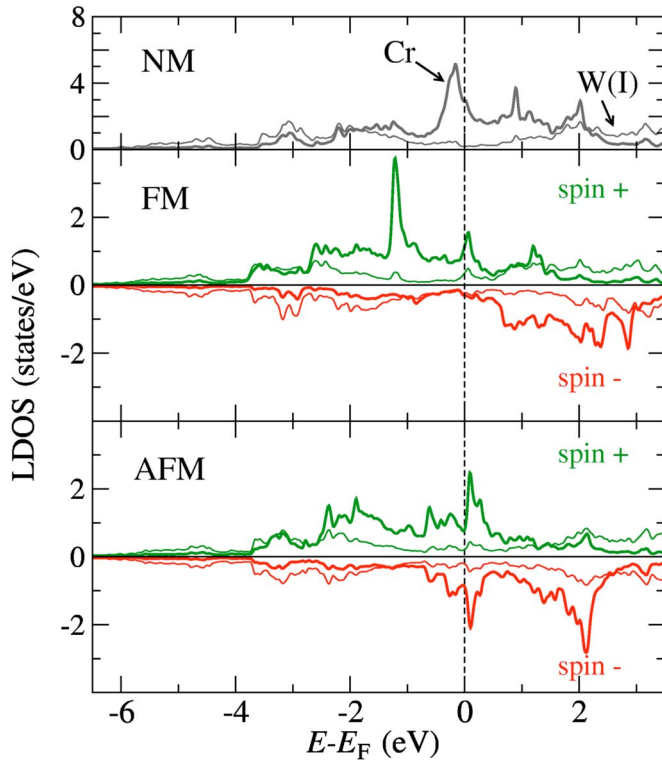


FIG. 3. (Color online) LDOS of 1 ML Cr on W(001) for (a) the nonmagnetic, (b) the FM, and (c) the AFM configuration. Thick (thin) lines denote the LDOS of the Cr (W interface) atoms.

strate: (i) the larger in-plane lattice constant of W as compared to Pd or (ii) the stronger hybridization of 3d TM monolayer with W with respect to the weakly interacting Pd.

In order to work this out we performed calculations for 3d TM UMLs in the experimental W lattice constant. The energy difference given in Fig. 2 shows the same trend as for 3d TM monolayers on Pd(001). However, the larger in-plane interatomic spacing in these UMLs as compared to Pd (15%) reduces the overlap between the 3d wave functions and lowers the energy differences for all 3d TMs. The V UML becomes FM. For V on Pd(001) where the AFM configuration is only a few meV/atom lower than the FM state, the different magnetic structure can be explained directly on the basis of the in-plane interatomic spacing. For the other 3d TM monolayers on W(001), we deduce that the unexpected magnetic order must be due to the 3d–5d hybridization between the TMs and W, i.e., $J_{\perp} \gg J_{\parallel}$. A closer look reveals a significant difference between a bcc substrate as W and a fcc substrate as Cu, Pd, Ag, or Au. For a bcc substrate each TM atom has four nearest W atoms at the interface, while the surrounding TM atoms in the overlayer are only next-nearest neighbor atoms. Considering that the 5d orbitals of W are more extended than the 3d ones of the overlayer and taking the additional interlayer relaxation into account, we can conclude that the overlayer–substrate interaction is more important than the interaction between 3d TM atoms in the monolayer plane and thus the nature of the 3d–5d bond will determine the physics.

In the following, we choose Cr and Co MLs on W(001) as the two most surprising examples on both sides of the trend

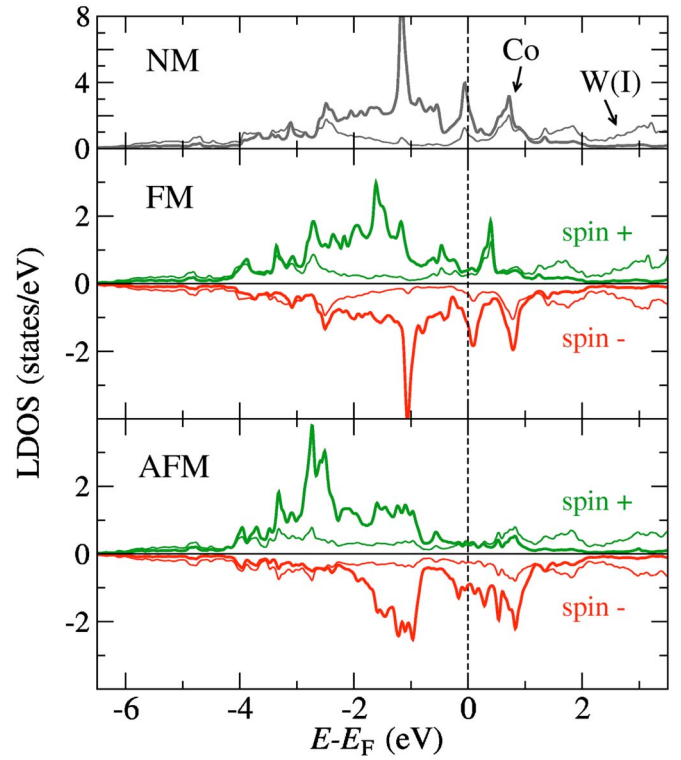


FIG. 4. (Color online) LDOS of 1 ML Co on W(001) for (a) the nonmagnetic, (b) the FM, and (c) the AFM configuration. Thick (thin) lines denote the LDOS of the Co (W interface) atoms.

to further investigate the cause of the unexpected magnetic order. The FM configuration of 1 ML Cr on W(001) seems unusual at first glance but can be understood on the basis of a comparison with the plain Cr(001) surface. The Cr(001) surface has a LAFM structure, i.e., FM coupling of atoms within each layer and an AFM coupling of atoms between adjacent layers.^{15,16} Since Cr and W have the same crystal structure and are in the same column of the periodic table, the Fermi surface and subsequently the magnetic susceptibilities are rather similar, which explains the FM order of the Cr monolayer and the LAFM coupling to the spin-polarized W substrate.

The interaction between the overlayer and the substrate, which is the origin of the unexpected magnetic order, can be inferred from the density of states (DOS) given in Fig. 3 for one ML Cr on W(001). The nonmagnetic local DOS (LDOS) of the Cr atoms, Fig. 3(a), shows three major peaks resulting from the crystal-field splitting of the *d* electrons in the C_{4v} symmetry of the square lattice for a (001) surface of a bcc crystal.¹⁷ Most features of the Cr LDOS appear at the same energy as in the LDOS of the W interface atoms, indicating a strong 3d–5d Cr–W hybridization. The only exception is the region of the W pseudogap close to the Fermi level. In the FM state, Fig. 3(b), the Cr LDOS has essentially the same shape as the nonmagnetic LDOS, with majority and minority bands shifted by the exchange interaction. In the AFM state, however, the mixing of spin up and down states from adjacent Cr atoms with antiparallel moments leads to a distinctively different shape of the LDOS depicted in Fig. 3(c). In both spin channels sharp peaks appear in the close vicinity of

the Fermi energy which are present also at W. These interface states are due to hybridization within the W pseudogap and resemble the W surface state.¹⁸ The lower total energy of the FM solution results from the larger exchange splitting, compared to the AFM case, which shifts the minority bands to higher energies and decreases their contribution to the total energy. In addition, the larger exchange in the FM state produces a higher magnetic moment with respect to the AFM one (cf. Fig. 1).

Let us analyze the case of 1 ML Co on W(001) next. Co is a prototypical ferromagnet and has never been predicted to become AFM. As we can see from the nonmagnetic LDOS, Fig. 4(a), the 3d band of Co is shifted to lower energy compared to Cr, due to the larger *d* band filling. In this case, an interface state appears already in the nonmagnetic case. For the Co monolayer, the exchange splitting (and consequently the magnetic moment) is much larger in the AFM state and the Fermi level lies well above the majority Co *d* band, which contributes no states close to the Fermi level. In the FM configuration, on the other hand, the interface state is present directly at the Fermi energy and accounts significantly to the total energy.

We conclude from the discussion of Cr and Co that the relative lineup of the TM 3d bands with the 5d bands of the W substrate is crucial in determining the magnetic order. In particular, the appearance of surface (interface) states at the Fermi energy supports the FM (AFM) order. The band lineup can be modified not only by changing the 3d band filling of the overlayer, but alternatively by varying the 5d band filling of the substrate. In principle, switching from W to Ta or Nb, which crystallize also in the bcc structure having a similar lattice constant as W, but with one *d* electron less, could lead to results with a different magnetic order across the 3d TM series. But this is a matter of future investigations.

The result of Fig. 2 is also surprising if we consider that the trend of the total energy difference across the 3d TM monolayer series is completely reversed for the case of a W(110) substrate, showing the same behavior as for noble metals and Pd. This is clearly a surface or interface effect. In

case of strong overlayer-substrate hybridization, the different coordination number, symmetry and interlayer distance is critical to the determination of the magnetic properties of the system. For the case of the (001) surface, each 3d-metal atom is in a C_{4v} environment with four W nearest neighbors. For the (110) surface, instead, the symmetry is C_{2v} and the number of W nearest neighbor is two. Moreover, the interlayer distance is much smaller for the (001) surface, making the hybridization with the substrate even stronger.

In summary, we have presented a systematic calculation for 3d transition-metal monolayers on W(001). We found a surprising trend for the magnetic order of 3d-metal monolayers on nonmagnetic (001) substrates: The FM configuration is the ground state for V, Cr, and Mn while the $c(2 \times 2)$ AFM state is more stable for Fe and Co. A Ni overlayer is nonmagnetic. We attribute the origin of this magnetic trend to the nature of the 3d–5d bond between the overlayer and the substrate. Changing the 3d band filling of the overlayer or the 5d band filling of the substrate shifts the relative position of both bands and alters the character of the 3d–5d bond which finally can result in a change of sign in the exchange interaction $J_{\perp}(3d-5d)$. The chemical trend discussed here for the W(001) substrate should also hold for Mo(001), but the magnetic order of 3d metals on other bcc(001) surfaces such as V, Nb, Ta is not yet clear. A possible tuning of the substrate *d* band filling by proper alloying could allow to control the competition between ferro- and antiferromagnetic interactions of the Fe monolayer and eventually bring about new complex magnetic structures not yet observed. The bcc(001) surfaces assure the presence of a d_{z^2} surface state¹⁹ that can be probed well by scanning tunneling spectroscopy. Probing these states can eventually provide evidence of the proposed magnetic order. The magnetic state can alternatively be observed directly in spin-polarized scanning tunneling microscopy images.⁸

S. B. thanks R. Robles for his help with the calculations of Cr on W(001). S. H. thanks the “Stifterverband für die Deutsche Wissenschaft” and the “Interdisciplinary Nano-science Center Hamburg for financial support.”

*Electronic address: pferrian@physnet.uni-hamburg.de

¹A. J. Freeman and A. Q. Wu, J. Magn. Magn. Mater. **100**, 497 (1991).

²T. Asada, G. Bihlmayer, S. Handschuh, S. Heinze, P. Kurz, and S. Blügel, J. Phys.: Condens. Matter **11**, 9347 (1999).

³S. Blügel, M. Weinert, and P. H. Dederichs, Phys. Rev. Lett. **60**, 1077 (1988).

⁴S. Blügel, Europhys. Lett. **9**, 597 (1989).

⁵J. E. Ortega and F. J. Himpsel, Phys. Rev. B **47**, 16441 (1993).

⁶S. Heinze, M. Bode, A. Kubetzka, O. Pietzsch, X. Nie, S. Blügel, and R. Wiesendanger, Science **288**, 1805 (2000).

⁷D. Spišák and J. Hafner, Phys. Rev. B **70**, 195426 (2004).

⁸A. Kubetzka, P. Ferriani, M. Bode, S. Heinze, G. Bihlmayer, K. von Bergmann, O. Pietzsch, S. Blügel, and R. Wiesendanger, Phys. Rev. Lett. **94**, 087204 (2005).

⁹W. Wulfhekel, T. Gutjahr-Löser, F. Zavaliche, D. Sander, and J. Kirschner, Phys. Rev. B **64**, 144422 (2001).

¹⁰M. Przybylski and U. Gradmann, Phys. Rev. Lett. **59**, 1152 (1987).

¹¹<http://www.flapw.de>.

¹²Y. Zhang and W. Yang, Phys. Rev. Lett. **80**, 890 (1998).

¹³M. Methfessel, D. Hennig, and M. Scheffler, Phys. Rev. B **46**, 4816 (1992).

¹⁴S. Handschuh and S. Blügel, Solid State Commun. **10**, 633 (1998).

¹⁵S. Blügel, D. Pescia, and P. H. Dederichs, Phys. Rev. B **39**, R1392 (1989).

¹⁶R. Wiesendanger, H. J. Güntherodt, G. Güntherodt, R. J. Gambino, and R. Ruf, Phys. Rev. Lett. **65**, 247 (1990).

¹⁷X. Qian and W. Hübner, Phys. Rev. B **67**, 184414 (2003).

¹⁸L. F. Mattheiss and D. R. Hamann, Phys. Rev. B **29**, 5372 (1984).

¹⁹J. A. Stroscio, D. T. Pierce, A. Davies, R. J. Celotta, and M. Weinert, Phys. Rev. Lett. **75**, 2960 (1995).